

# Photo- and radio-luminescence properties of 3CaO-2SiO<sub>2</sub> and 3CaF<sub>2</sub>-2SiO<sub>2</sub> glasses doped by Ce<sup>3+</sup> ions

Y. Tratsiak<sup>a,b</sup>, E. Trusova<sup>c,b</sup>, G. Dosovitsky<sup>d</sup>, M. Fasoli<sup>e</sup>, M. Korjik<sup>b,d</sup>, F. Moretti<sup>e</sup>, A. Vedda<sup>e,\*</sup>

<sup>a</sup>Research Institute for Physical Chemical Problems, Belarusian State University,  
Leningradskaya str. 14, 220030 Minsk, Belarus

<sup>b</sup>Research Institute for Nuclear Problems, Belarusian State University, Bobruiskaya str. 11,  
220030 Minsk, Belarus

<sup>c</sup>Belarusian State Technological University, Sverdlova str. 13a, 220006 Minsk, Belarus

<sup>d</sup>National Research Center "Kurchatov Institute", Moscow, Russia

<sup>e</sup>Department of Materials Science, University of Milano-Bicocca, Via R. Cozzi 55, 20125  
Milano, Italy

---

## Abstract

Wavelength-shifting materials in the form of optical fibers are requested in order to both convert UV scintillation light produced by fast scintillators into a more easily detectable visible light, and to efficiently transport it to the detectors.

In the present investigation we have considered glasses with composition 3CaO-2SiO<sub>2</sub> and 3CaF<sub>2</sub>-2SiO<sub>2</sub> doped with 0.05, 0.5 and 1 at. % of Ce<sup>3+</sup> ions, prepared by an original method consisting in a combination of co-precipitation and sol-gel approaches. The glasses have been investigated by Raman scattering, as well as by photo- and radio-luminescence.

The glasses are characterized by complex Raman features. Composite photo-luminescence excitation and emission spectra are also detected in all cases, depending upon glass composition and Ce concentration. Broad excitation spectra extend from approximately 260 nm to 360 nm, while the composite Ce<sup>3+</sup> emission is detected in the blue spectral region at around 400 nm. A satisfactory matching between the excitation spectra of the glasses and the emission spectrum of CeF<sub>3</sub> scintillator occurs, confirming their potential application as wavelength shifters of CeF<sub>3</sub> UV scintillation light. Moreover, bright photo-luminescence signals are accompanied by a very poor radio-luminescence. The results are discussed by taking into account the presence of different silicate clusters embedded in the glass network, as well as the role of point defects in the radio-luminescence process.

**Keywords:** Glasses; luminescence; scintillations

---

\*Corresponding author

Email address: E-mail: [anna.vedda@unimib.it](mailto:anna.vedda@unimib.it) (A. Vedda)

## 1. Introduction

A great variety of single crystals possess favorable properties as scintillators materials, like high luminescence efficiency coupled to a small amount of defects and traps that could influence the carrier recombination process. Nonetheless, crystals have also a number of disadvantages that sometimes limits their application. In fact, they often have a high cost, due to the expensive equipments for their production, slow and expensive growth. The growth of large crystals is also a challenge. The search of alternatives to single crystals for application in ionizing radiation detectors is therefore an important task [1, 2, 3, 4, 5].

Besides crystalline materials, there are a great number of other inorganic materials that can be promising scintillators, specifically, glasses. The main origin for their often poor scintillation is their disordered structure, which leads to the formation of a great number of traps, competing with luminescent ions in free carrier capture. On the other hand, glasses can be obtained with a wide variety of compositions, and moreover glass-ceramics can also be prepared thanks to a partial crystallization of the network [6, 7]. Such versatility encourages their development through controlled preparation techniques and suitable doping.

Among glassy materials, silicates look to be the most promising hosts for developing new phosphors. Silica is a glass forming compound. Moreover, silicates in the crystalline phase find numerous application as luminescent materials. Single-crystalline  $(RE)_2SiO_5$  and  $(RE)_2Si_2O_7$  silicates ( $RE = Lu, Y, Gd$ ) doped with  $Ce^{3+}$  are good scintillating materials [8, 9, 10, 11]. Similarly to single crystals, some silicate glasses show bright near UV or blue luminescence. For example, lithium silicate glass is widely used as neutron sensitive scintillating sensors [12]. Glass and glass ceramics made of stoichiometric  $Li_2O-2SiO_2$  composition possess a light yield better than 7000 ph/n [13]. Glass made of stoichiometric  $BaO-2SiO_2$  composition features a high photo-luminescence quantum efficiency, scintillation light yield at the level of 1000 ph/MeV, and good hardness after irradiation with gamma rays and 150 MeV protons [7, 14]. These features make silicate stoichiometric glasses promising materials in fiber or bulk form for nuclear instrumentation. For example, silica fiber sensors doped with  $Ce^{3+}$  or  $Yb^{3+}$  ions are being investigated for real time remote dosimetry in medical diagnostic and therapy [15, 16].

Moreover, recently particular interest for glasses was raised by their application potential to act, in fiber form, as wavelength shifters (WLS) of UV scintillation light emitted for example by  $CeF_3$  and  $BaF_2$  [17, 18] and neutron sensitive Li-Si-Al scintillation glass emitting in a near UV range [19]. Their scope is to transform UV emitted light in a more easily detectable visible emission, and simultaneously provide its transport to the detector. At variance with other applications, in this case the material has to possess a low density and a poor scintillation yield. These features make such type WLS fibers to be not sensitive to ionizing radiation and exclude their contribution in the signals of the detecting units, which is particularly important in high energy physics experiments.

To the purpose of developing wavelength shifting materials, we considered

Table 1: Glass samples names, their compositions and  $\text{Ce}^{3+}$  ions concentrations

Short name	Composition	$\text{Ce}^{3+}$ ions concentration, at. % of $\text{Ca}^{2+}$ ions
CaO005	$3\text{CaO}\cdot 2\text{SiO}_2$	0.05
CaO05	$3\text{CaO}\cdot 2\text{SiO}_2$	0.5
CaO1	$3\text{CaO}\cdot 2\text{SiO}_2$	1
CaF005	$3\text{CaF}_2\cdot 2\text{SiO}_2$	0.05
CaF05	$3\text{CaF}_2\cdot 2\text{SiO}_2$	0.5
CaF1	$3\text{CaF}_2\cdot 2\text{SiO}_2$	1

glasses with  $3\text{CaO}\cdot 2\text{SiO}_2$  composition. Moreover, we also report the effect of partial substitution of oxygen ions by fluorine ions on luminescent properties of  $\text{Ce}^{3+}$  ions in a calcium silicate glass system with  $3\text{CaF}_2\cdot 2\text{SiO}_2$  composition. As described below, we used a complex method consisting in a combination of  
50 co-precipitation and sol-gel approaches, to produce glass precursors.

## 2. Materials and Methods

$\text{Ce}(\text{NO}_3)_3\cdot 6\text{H}_2\text{O}$ ,  $\text{NH}_4\text{F}$ , TEOS, ethanol,  $\text{Ca}(\text{NO}_3)_2\cdot 4\text{H}_2\text{O}$ ,  $\text{NH}_4\text{HCO}_3$  were used as starting materials. All reactants were analytical grade.

Two different kinds of glasses with different  $\text{Ce}^{3+}$  concentrations,  $3\text{CaO}\cdot 2\text{SiO}_2\text{:Ce}$  and  $3\text{CaF}_2\cdot 2\text{SiO}_2\text{:Ce}$ , were obtained. The main difference between  
55 glasses lies in using different calcium compounds doped by  $\text{Ce}^{3+}$  ions, obtained by co-precipitation method  $\text{CaF}_2\text{:Ce}$  for  $3\text{CaF}_2\cdot 2\text{SiO}_2\text{:Ce}$  glasses and  $\text{CaCO}_3\text{:Ce}$  for  $3\text{CaO}\cdot 2\text{SiO}_2\text{:Ce}$  glasses.

$\text{CaCO}_3\text{:Ce}$  has been obtained by co-precipitation of mixed water solution of  
60  $\text{Ca}(\text{NO}_3)_2$  and  $\text{Ce}(\text{NO}_3)_3$  into water solution of  $\text{NH}_4\text{HCO}_3$ .  $\text{CaF}_2\text{:Ce}$  has been obtained by co-precipitation of mixed water solution of  $\text{Ca}(\text{NO}_3)_2$  and  $\text{Ce}(\text{NO}_3)_3$  into water solution of  $\text{NH}_4\text{F}$ . The quantity of  $\text{Ce}(\text{NO}_3)_3$  corresponds to substitution of 0.05, 0.5 or 1 at. % of  $\text{Ca}^{2+}$  ions by  $\text{Ce}^{3+}$  ions. Isolated precipitates of  $\text{CaCO}_3\text{:Ce}$  and  $\text{CaF}_2\text{:Ce}$  have been introduced into water-alcohol solution of  
65 TEOS, which has then been subjected to alkaline hydrolysis. The obtained gels of precursors of  $3\text{CaO}\cdot 2\text{SiO}_2\text{:Ce}$  and  $3\text{CaF}_2\cdot 2\text{SiO}_2\text{:Ce}$  glasses were dried in air at  $80^\circ$ . The resulting xerogels (in powder form) were melted in a Falorni gas oven in  $\text{ZrO}_2/\text{Al}_2\text{O}_3$  crucibles at  $1500^\circ\text{C}$  for 3 hours. To avoid crystallization during cooling, the glasses were casted on non-preheated steel blocks and subsequently treated in a Nabertherm LHT 18/04 muffle furnace preheated at  $580^\circ\text{C}$   
70 to reduce mechanical stresses. The obtained glass blocks were transparent and colorless. For optical measurements, specimens with thickness 1 mm were cut and polished. Samples short names and their composition are listed in Table 1.

Some comparisons were performed with a sol-gel  $\text{SiO}_2\text{:}0.1$  mol. %  $\text{Ce}^{3+}$  ions  
75 sample sintered in reducing conditions [20], and with a  $\text{CeF}_3$  single crystal.

X-ray excited radio-luminescence (RL) measurements were carried out with a homemade apparatus featuring a CCD detector (Jobin-Yvon Spectrum One 3000) coupled to a monochromator (Jobin-Yvon Triax 180) with a 300 grooves/mm

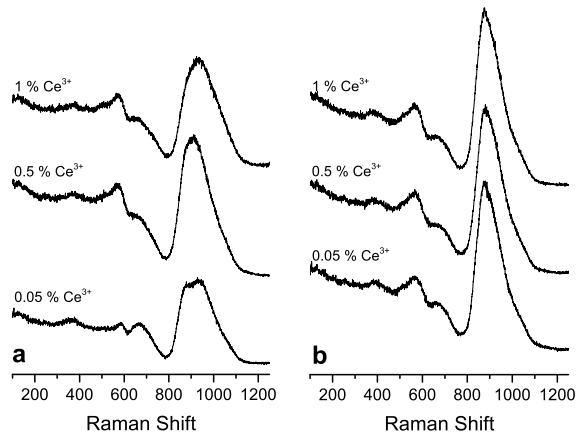


Figure 1: Raman spectra of CaO-SiO<sub>2</sub>:Ce(a) and CaF<sub>2</sub>-SiO<sub>2</sub>:Ce(b) glasses

grating. RL was excited by X-ray irradiation using a Philips 2274 tube oper-  
 80 ating at 20 kV and 20 mA. All X-ray irradiations were carried out in the same  
 conditions varying only the exposition time.

For optical absorption a Varian Cary 50 spectrophotometer was used. The  
 optical absorption spectra were acquired in the 190-1100 nm wavelength range.

Steady state photoluminescence (PL) spectra were measured using a xenon  
 85 lamp as excitation source, followed by a double monochromator (Jobin-Yvon  
 Gemini 180 with a 1200 grooves/mm grating), and recorded by a nitrogen cooled  
 CCD detector coupled to a monochromator (Jobin-Yvon Micro HR).

Raman measurements were performed in backscattering configuration with a  
 frequency doubled Nd:YAG laser as excitation source ( $\lambda = 532$  nm) on a Jobin-  
 90 Yvon T64000 triple monochromator equipped with a liquid nitrogen cooled  
 CCD (Jobin-Yvon Symphony). The measurements detection range was 100-  
 3500 cm<sup>-1</sup>.

All measurements were performed at room temperature (RT).

### 3. Experimental Results and Discussion

95 The Raman spectra of alkali-earth silicate glasses are discussed in detail in  
 [21, 22, 23, 24, 25]. In general, the Raman spectra of investigated glasses seem  
 to be similar and their differences mainly consist in the relative intensities of  
 the bands (Fig. 1).

100 The most intense signal is located between 800 and 1150 cm<sup>-1</sup> and it consists  
 of a broad unresolved and asymmetric structure featuring principal components  
 with maxima at around 875 cm<sup>-1</sup> and 910-935 cm<sup>-1</sup>. The band at 875 cm<sup>-1</sup>  
 could be assigned to symmetric stretching vibrations of non-bridging oxygen

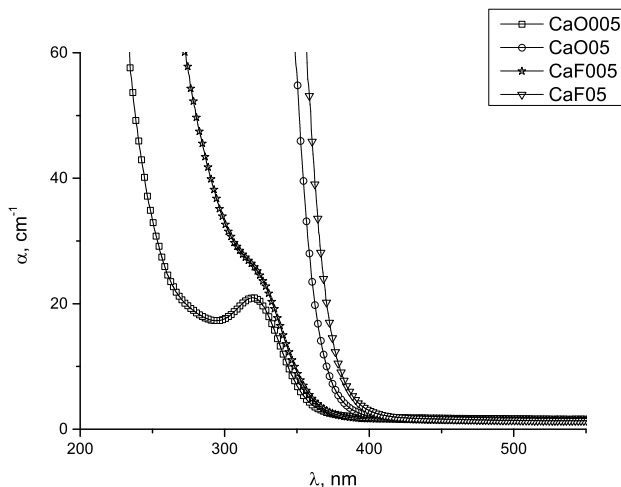


Figure 2: Optical absorption spectra of CaO005, CaO05, CaF005 and CaF05

bonds in separate  $\text{SiO}_4^{4-}$  tetrahedra in the orthosilicate structure [22]. The band with maximum at  $910\text{-}935\text{ cm}^{-1}$ , in principle, can be associated to two kinds of vibrations. It can correspond to  $\text{Si}_2\text{O}_7^{6-}$  vibrations in the pyrosilicate structure, or to the presence of  $(\text{SiO}_4)_n^{2-}$  chains [23, 25]. The band located above  $1000\text{ cm}^{-1}$  (it looks like a weak shoulder in both families of samples) could correspond to the anti-symmetric stretching vibration in a three-dimensional array of  $\text{SiO}_4$  tetrahedra [22]. The weak broad band at  $650\text{-}660\text{ cm}^{-1}$  can be assigned to Si-O-Si linkages and asymmetric stretching vibrations of bridging oxygen bonds in crystalline pyrosilicates [22]. Moreover, the band at  $575\text{-}580\text{ cm}^{-1}$  could correspond to bending motions of oxygen bonds in direct structures in quenched  $\text{SiO}_2$  [25]. The broad structure located between  $100$  and  $500\text{ cm}^{-1}$  contains the contribution from the rocking mode of silica at  $440\text{ cm}^{-1}$  [25, 26, 27].

In general, substitution of  $\text{O}^{2-}$  with  $\text{F}^-$  should distort the electronic environment of silica because of the higher electronegativity of  $\text{F}^-$  compared to the  $\text{O}^{2-}$  one. This distortion could weaken the remaining Si-O bonds in the silica tetrahedron, decreasing the force constants and the vibrational frequencies involving these Si-O bonds. As a result, increasing the  $\text{F}^{2-}$ -to- $\text{O}^{2-}$  ratio in  $\text{SiO}_x\text{F}_y$  compound is expected to decrease the frequency of the resultant bands in the Raman spectrum up to  $\sim 50\text{ cm}^{-1}$  per oxygen replaced by  $\text{F}^-$  [28]. However in the investigated samples the Raman spectra are similar, and only relative bands intensity differences are observed. This indicates a weak influence of  $\text{F}^-$  on the glass network, possibly due to the fact that fluorine ions are predominantly coordinated near  $\text{Ca}^{2+}$  ions [21, 28].

The optical absorption spectra of CaO005, CaO05, CaF005 and CaF05 glasses are in Fig. 2.

A partially unresolved peak at  $320\text{ nm}$  is observed for CaO005 sample. It is

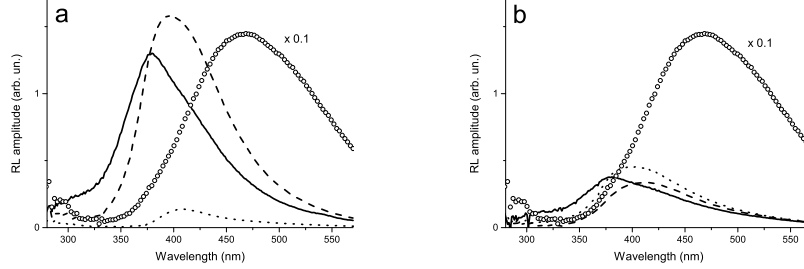


Figure 3: RL spectra of glasses with composition  $3\text{CaO}\cdot 2\text{SiO}_2$  (a) and  $3\text{CaF}_2\cdot 2\text{SiO}_2$  (b) with 0.05 (solid line), 0.5 (dashed line) and 1 (dotted line) at. % of  $\text{Ce}^{3+}$  ions in comparison with BGO (marked as circles, spectrum is multiplied by 0.1)

manifested as a shoulder for the CaF005 sample. This peak corresponds to the  
 130 lowest  $4f\text{-}5d^1$  inter-configuration transition of  $\text{Ce}^{3+}$ . Increasing the concentration  
 of  $\text{Ce}^{3+}$  ions strongly increases this absorption and only its long wavelength  
 tail could be measured in samples with 0.5 at. % Ce (CaO05 and CaF05). In  
 low- $\text{Ce}^{3+}$  samples, at wavelengths below 300 nm a very strong absorption in-  
 crease is detected. The origin of this absorption deserves further investigations,  
 135 taking into account the role of charge compensating defects due to the presence  
 of  $\text{Ca}^{2+}$  and  $\text{F}^-$  in the silica network.

The RL spectra of the investigated samples are presented in Fig.3.

The RL spectra shape depends on  $\text{Ce}^{3+}$  concentration. All the emissions  
 consist of unresolved  $5d^1\text{-}^2\text{F}_{5/2}$  and  $5d^1\text{-}^2\text{F}_{7/2}$  radiating transitions of  $\text{Ce}^{3+}$ . For  
 140 CaO005 and CaF005, the emission peak is at approximately 380 nm. Increasing  
 the  $\text{Ce}^{3+}$  concentration leads to a red shift: up to  $\sim 395$  and  $\sim 410$  nm for CaO05  
 and CaF05 samples respectively, and up to  $\sim 405$  and 400 nm for CaO1 and  
 CaF1 samples respectively. The red shift is probably related to the absorption  
 spectra modifications displayed in Fig.2: in other words, it might be an effect  
 145 of a stronger re-absorption of the short wavelength side of the luminescence  
 emission band.

The intensity difference of the RL spectra for  $3\text{CaO}\cdot 2\text{SiO}_2$  and  $3\text{CaF}_2\cdot 2\text{SiO}_2$   
 samples can be explained by the difference in their anionic surrounding. Partial  
 substitution of oxygen ions by fluorine ions can contribute to the increase of the  
 150 number of defects that work as traps and lead to a decrease of the scintillation  
 efficiency.

Photo-luminescence excitation spectra (for 420 nm emission) are presented  
 in Fig. 4. For all  $3\text{CaO}\cdot 2\text{SiO}_2$  and  $3\text{CaF}_2\cdot 2\text{SiO}_2$  samples the spectra consist of  
 several unresolved bands, also influenced by the  $\text{Ce}^{3+}$  content.

155 Excitation spectra extend from approximately 260 nm to 390 nm. A stronger  
 contribution at wavelengths below 300 nm is detected for  $3\text{CaO}\cdot 2\text{SiO}_2$  with re-  
 spect to  $3\text{CaF}_2\cdot 2\text{SiO}_2$ . For  $3\text{CaO}\cdot 2\text{SiO}_2\text{:Ce}$  glasses the long wavelength excita-  
 tion part (corresponding to the  $4f\rightarrow 5d^1$  transition of  $\text{Ce}^{3+}$ ) displays a red shift  
 with increasing  $\text{Ce}^{3+}$  concentration from 335 nm (sample CaO005) to 355 nm

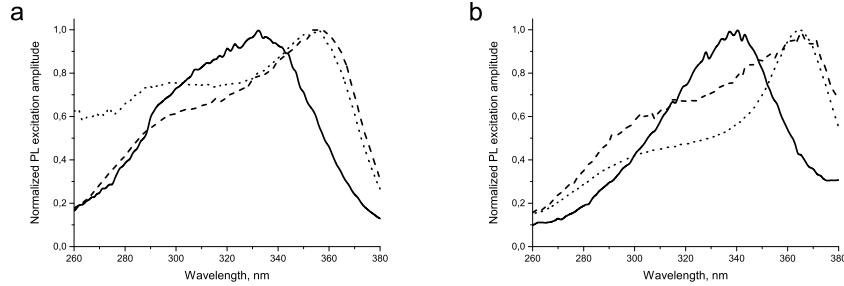


Figure 4: Normalized excitation spectra for  $3\text{CaO}\cdot 2\text{SiO}_2\text{:Ce}$  (a) and  $3\text{CaF}_2\cdot 2\text{SiO}_2\text{:Ce}$  (b) glasses with 0.05 (solid line), 0.5 (dashed line) and 1 (dotted line) at. % of  $\text{Ce}^{3+}$  ions

160 (samples CaO05 and CaO1). The same phenomenology is observed in  $3\text{CaF}_2\cdot 2\text{SiO}_2\text{:Ce}$  samples: the long wavelength part of the band is shifted from 340 nm (sample CaF005) to 365 nm (samples CaF05 and CaF1). This effect is most probably due to the high light absorption level while  $\text{Ce}^{3+}$  concentration is increased.

165 PL emission spectra at different excitation wavelengths (300 nm, and 360 nm) are reported in Fig. 5.

For both kind of glasses, remarkable spectral shifts are observed as a function of excitation wavelength and  $\text{Ce}^{3+}$  concentration. For example, under 300 nm or 360 nm excitation, the emission peak positions of CaO005 result to be 385 nm and 420 nm respectively. In general, the presence of different emission peaks can be the result of the presence of  $\text{Ce}^{3+}$  ions in different surroundings. This is also suggested by Raman data that reveal the occurrence of vibrations related to different silicate structures. With the increase of the  $\text{Ce}^{3+}$  content, part of them are localized in new different surroundings. The comparison between 175 PL and RL spectra demonstrates that the center responsible for the emission excited at 300 nm gives a major contribution under ionizing radiation excitation. Interestingly, in two cases (Fig. 5 c, f) the RL occurs at still lower wavelengths with respect to PL, indicating the presence of a third kind of cerium center that was not evidenced in our PL experiments.

180 Weak RL intensities and bright PL emissions with UV excitation in a wide spectral range make these glasses interesting materials as wavelength shifters in combination with UV emitting scintillators, for example  $\text{CeF}_3$  or Ce-doped Li-Si-Al scintillating glasses. In order to qualitatively display such characteristic, a comparison between PL and RL intensities of  $3\text{CaO}\cdot 2\text{SiO}_2$  with 0.5 %  $\text{Ce}^{3+}$  and sol-gel  $\text{SiO}_2$ : 0.1 mol % Ce sintered in reducing conditions [20] is shown in 185 Fig. 6.

The PL intensity for CaO05 is 3 times lower than that of  $\text{SiO}_2\text{:Ce}$  glass, while the RL intensity of CaO05 is lower than that of  $\text{SiO}_2\text{:Ce}$  glass by more than two orders of magnitude. Similar results occur also for the other glass 190 compositions investigated.

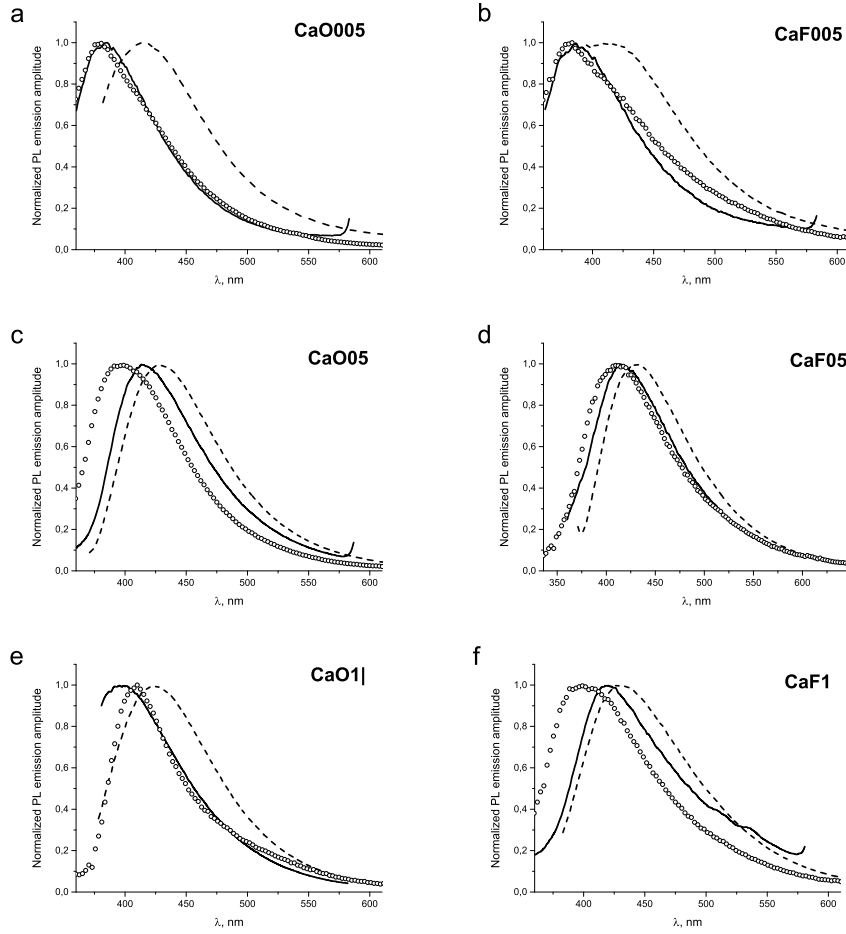


Figure 5: Normalized PL emission spectra obtained with excitation at 300 nm (solid line) and 360 nm (dashed line) for  $3\text{CaO}-2\text{SiO}_2$  (a, c, e) and  $3\text{CaF}_2-2\text{SiO}_2$  (b, d, f) glasses with 0.05 (a, b), 0.5 (c, d) and 1 (e, f) at. % of  $\text{Ce}^{3+}$  ions in comparison with their normalized RL spectra (marked by circles)



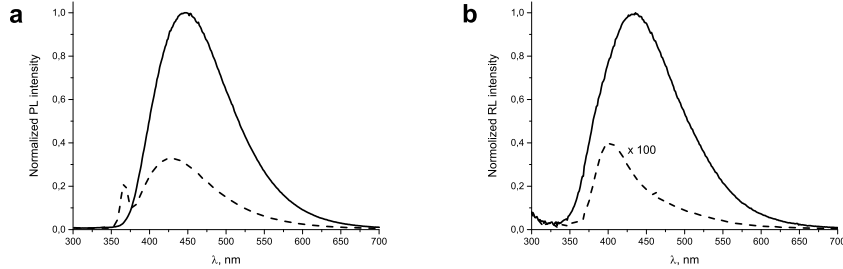


Figure 6: Comparison between PL (panel (a)) and RL (panel (b)) measurements of sol-gel  $\text{SiO}_2$ : 0.1 % Ce (solid lines) and CaO05 (dashed lines). Data are normalized with respect to sol-gel  $\text{SiO}_2$ :Ce. In panel (b) the RL curve of  $3\text{CaO}-2\text{SiO}_2$  glass is multiplied by 100. For PL,  $\lambda_{\text{exc}}$  were 350 nm for  $\text{SiO}_2$ :Ce glass and 360 nm for CaO05.

Fig. 7 displays the satisfactory spectral overlap between  $\text{CeF}_3$  RL emission and the PLE excitation bands of CaO1 respectively. Such overlap allows  $3\text{CaO}-2\text{SiO}_2$ :Ce glass to absorb efficiently the UV light emitted by  $\text{CeF}_3$  converting it in the blue spectral region.

#### 195 4. Conclusions

$3\text{CaO}-2\text{SiO}_2$  and  $3\text{CaF}_2-2\text{SiO}_2$  glasses doped with different  $\text{Ce}^{3+}$  concentrations have been produced using an original method consisting in a combination of co-precipitation and sol-gel approaches. Their optical properties have been investigated in order to explore their potential application as wavelength shifters coupled to a UV-emitting scintillator, transforming the UV scintillation light into a more easily detectable visible emission. Moreover, fibers drawn from these materials could allow a more effective scintillation light extraction in detectors with complex geometries.

Bright and composite photoluminescence emissions around 430 nm are observed in all samples, characterized by broad excitation spectra extending from approximately 260 to 390 nm. The excitation spectra well match the emission spectrum of  $\text{CeF}_3$  and Li-Si-Al scintillation glass; such matching proves the capability of the glasses to act as wavelength shifters thanks to their strong absorption of UV scintillation, and its conversion into a longer wavelength radiation. Moreover, very weak radio-luminescence signals are displayed by all samples. The different behaviors of the glasses during intra-center or above-band-gap excitations can be explained by taking into account the presence of defects in the glasses, affecting the transport stage of scintillation. This results in a different involvement of the host matrix during the two kinds of experiments. In fact, during irradiation with ionizing radiation the free carriers experience a significant migration in the host prior to be localized at luminescent centers ( $\text{Ce}^{3+}$  in our case). During such migration path, they can be trapped by defects which

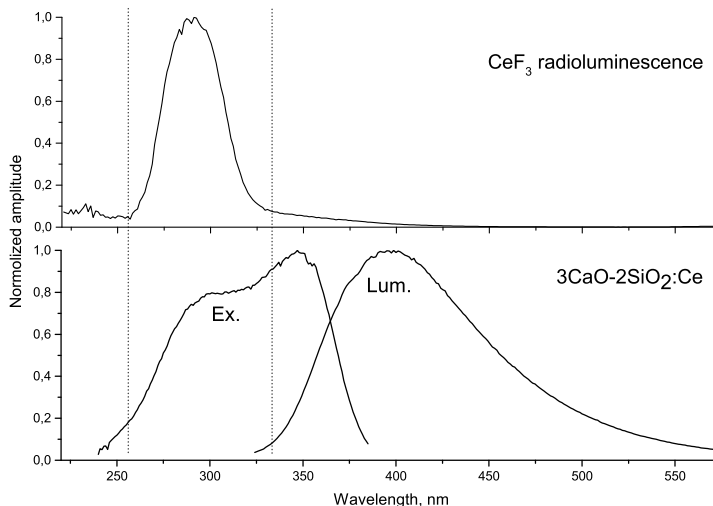


Figure 7: Upper panel, RL of  $\text{CeF}_3$  crystal; lower panel, PLE ( $\lambda_{\text{em}} = 400 \text{ nm}$ ) and PL ( $\lambda_{\text{ex}} = 300 \text{ nm}$ ) of  $\text{CaO}$  glass

prevent their final radiative recombination. Defects can also promote non radiative recombinations. Such processes are reasonably also related to the complex disordered glass structure, containing cations with different valence like  $\text{Ca}^{2+}$  and  $\text{Si}^{4+}$ . We do not exclude that high concentration of  $\text{Ca}^{2+}$  in the glass host also promotes fast non-radiative recombination of the free carriers created by ionizing radiation, as suggested by preliminary results obtained on other binary glasses with heavier alkaline earth ions like  $\text{Ba}^{2+}$  and  $\text{Sr}^{2+}$ . The involvement of defects is much less significant under intra-center excitation, resulting in bright photoluminescence emission in spite of a poor scintillation efficiency.

The favorable optical properties displayed by the considered glasses open the way for their future development in fiber form, to be employed in scintillation detectors as wavelength shifters.

### Acknowledgements

The collaboration and research were supported by the H2020 RISE Intelum Project (Grant Agreement 644260), the support of the grant No 14.W03.31.0004 of Ministry of Science and Education of Russian Federation also is appreciated.

### References

- [1] G. Blasse, Scintillator materials, *Chemistry of Materials* 6 (9) (1994) 1465–1475. doi:10.1021/cm00045a002.
- [2] D. J. Singh, Optical properties of halide and oxide scintillators, *Proc. SPIE* 8142 (2011) 81420U–81420U–7.

- 240 [3] M. Osinski, Emerging nanomaterials for nuclear radiation detectors, MRS Proceedings 1051. doi:10.1557/PROC-1051-CC01-06.
- [4] W. W. Moses, Current trends in scintillator detectors and materials, Nuclear Instruments and Methods in Physics Research Section A: Accelerators, Spectrometers, Detectors and Associated Equipment 487 (12) (2002) 123 – 128, 3rd International Workshop on Radiation Imaging Detectors.
- 245 [5] M. Nikl, A. Yoshikawa, Recent r&d trends in inorganic single-crystal scintillator materials for radiation detection, Advanced Optical Materials 3 (4) (2015) 463–481.
- [6] D. de Faoite, L. Hanlon, O. Roberts, A. Ulyanov, S. McBreen, I. Tobin, K. T. Stanton, Development of glass-ceramic scintillators for gamma-ray astronomy, Journal of Physics: Conference Series 620 (1) (2015) 012002.
- 250 [7] E. Auffray, N. Akchurin, A. Benaglia, A. Borisevich, C. Cowden, J. Damgov, V. Dormenev, C. Dragoiu, P. Dudero, M. Korjik, D. Kozlov, S. Kunori, P. Lecoq, S. W. Lee, M. Lucchini, V. Mechinsky, K. Pauwels, Dsb:ce<sup>3+</sup> scintillation glass for future, Journal of Physics: Conference Series 587 (1) (2015) 012062.
- 255 [8] D. Pauwels, N. L. Masson, B. Vianna, A. Kahn-Harari, E. V. D. van Loef, P. Dorenbos, C. W. E. van Eijk, A novel inorganic scintillator: Lu<sub>2</sub>Si<sub>2</sub>O<sub>7</sub>:ce<sup>3+</sup> (lps), in: 1999 IEEE Nuclear Science Symposium. Conference Record. 1999 Nuclear Science Symposium and Medical Imaging Conference (Cat. No.99CH37019), Vol. 1, 1999, pp. 102–105 vol.1. doi:10.1109/NSSMIC.1999.842456.
- 260 [9] L. Pidol, A. Kahn-Harari, B. Viana, B. Ferrand, P. Dorenbos, J. T. M. de Haas, C. W. E. van Eijk, E. Virey, Scintillation properties of lu<sub>2</sub>si<sub>2</sub>o<sub>7</sub>:ce<sup>3+</sup>, a fast and efficient scintillator crystal, Journal of Physics: Condensed Matter 15 (12) (2003) 2091.
- 265 [10] H. Feng, D. Ding, H. Li, S. Lu, S. Pan, X. Chen, G. Ren, Growth and luminescence characteristics of cerium-doped yttrium pyrosilicate single crystal, Journal of Alloys and Compounds 489 (2) (2010) 645 – 649.
- [11] J. Chen, L. Zhang, R.-Y. Zhu, Large size lyso crystals for future high energy physics experiments, IEEE Transactions on Nuclear Science 52 (6) (2005) 3133–3140. doi:10.1109/TNS.2005.862923.
- 270 [12] A. Spowart, Neutron scintillating glasses: Part 1, Nuclear Instruments and Methods 135 (3) (1976) 441 – 453.
- 275 [13] P. Lecoq, A. Gektin, M. Korzhik, Inorganic Scintillators for Detector Systems: Physical Principles and Crystal Engineering, Particle Acceleration and Detection, Springer International Publishing, 2016.

- [14] A. Borisevich, V. Dormenev, M. Korjik, D. Kozlov, V. Mechinsky, R. W. Novotny, Optical transmission radiation damage and recovery stimulation of dsb:ce<sup>3+</sup> inorganic scintillation material, *Journal of Physics: Conference Series* 587 (1) (2015) 012063. 280
- [15] A. Vedda, N. Chiodini, D. D. Martino, M. Fasoli, S. Keffer, A. Lauria, M. Martini, F. Moretti, G. Spinolo, M. Nikl, N. Solovieva, G. Brambilla, Ce<sup>3+</sup>-doped fibers for remote radiation dosimetry, *Applied Physics Letters* 85 (26) (2004) 6356–6358. doi:10.1063/1.1840127.
- [16] I. Veronese, C. D. Mattia, M. Fasoli, N. Chiodini, E. Mones, M. C. Cantone, A. Vedda, Infrared luminescence for real time ionizing radiation detection, *Applied Physics Letters* 105 (6) (2014) 061103. doi:10.1063/1.4892880. 285
- [17] B. Bilki, D. Winn, Y. Onel, New radiation-hard wavelength shifting fibers, in: *IEEE 2016 NSS/MIC*, 2016, pp. N29–52.
- [18] F. Micheli, P. Meridiani, R. Becker, L. Bianchini, G. Dissertori, M. Donegi, L. Brianza, D. D. Re, N. Chiodini, N. Pastrone, G. D. Ricca, N. Akchurin, M. Droge, C. Haller, U. Horisberger, T. Klijnsma, W. Lustermaun, A. Marini, D. Meister, Energy resolution and timing performance studies of a w-cef<sub>3</sub> sampling calorimeter with a wavelength-shifting fiber readout, in: *IEEE 2016 NSS/MIC*, 2016, pp. N40–2. 290 295
- [19] Saint gobain crystals catalogue (2017).  
URL <http://www.crystals.saint-gobain.com>
- [20] M. Fasoli, A. Vedda, A. Lauria, F. Moretti, E. Rizzelli, N. Chiodini, F. Meinardi, M. Nikl, Effect of reducing sintering atmosphere on ce-doped solgel silica glasses, *Journal of Non-Crystalline Solids* 355 (1821) (2009) 1140 – 1144. 300
- [21] Y. Sasaki, M. Iguchi, M. Hino, The estimation of the iso-viscosity lines in molten ca<sub>2</sub>-cao-sio<sub>2</sub> system, *ISIJ International* 47 (2) (2007) 346–347.
- [22] P. McMillan, Structural studies of silicate glasses and melts-applications and limitations of raman spectroscopy, *American Mineralogist* 69 (1969) 622–644. 305
- [23] Y. Tsunawaki, N. Iwamoto, T. Hattori, A. Mitsuishi, Analysis of cao-sio<sub>2</sub> and cao-sio<sub>2</sub>-ca<sub>2</sub> glasses by raman spectroscopy, *Journal of Non-Crystalline Solids* 44 (2) (1981) 369 – 378.
- [24] Y. Q. Wu, G. C. Jiang, J. L. You, H. Y. Hou, H. Chen, K. D. Xu, Theoretical study of the local structure and raman spectra of cao-sio<sub>2</sub> binary melts, *The Journal of Chemical Physics* 121 (16) (2004) 7883–7895. 310
- [25] B. O. Mysen, D. Virgo, C. M. Scarfe, Relations between the anionic structure and viscosity of silicate melts a raman spectroscopic study, *American Mineralogist* 65 (1980) 690–710. 315

- [26] R. J. Bell, P. Dean, Atomic vibrations in vitreous silica, *Discuss. Faraday Soc.* 50 (1970) 55–61.
- [27] A. Vedda, N. Chiodini, M. Fasoli, A. Lauria, F. Moretti, D. D. Martino, A. Baraldi, E. Buffagni, R. Capelletti, M. Mazzera, P. Bohacek, E. Mihokova, Evidences of rare-earth nanophases embedded in silica using vibrational spectroscopy, *IEEE Transactions on Nuclear Science* 57 (3) (2010) 1361–1369. doi:10.1109/TNS.2010.2044420.
- [28] R. W. Luth, Raman spectroscopic study of the solubility mechanisms of f in glasses in the system  $\text{CaO-CaF}_2\text{-SiO}_2$ , *American Mineralogist* 73 (1988) 297–305.